EPR and ENDOR of cubic ZnS: Mn^{2+}

R. de Beer and F. Biesboer

Department of Physics, Technische Hogeschool Delft, The Netherlands

G. van Veen

Laboratory of Physical Chemistry, Technische Hogeschool Delft, The Netherlands

(Z. Naturforsch. **32 a**, 724–730 [1977]; received May 27, 1977)

The spin Hamiltonian parameters of $^{55}Mn^{2+}$ in cubic ZnS have been determined by means of EPR and central-ion ENDOR, using Ka-band (35 GHz) microwaves. For the first time a value for the spherical electric quadrupole interaction of Mn^{2+} incorporated in a single crystal has been found. Also the ligand hyperfine interaction and the electric quadrupole interaction of the twelve Zn^{67} nuclei nearest to Mn^{2+} have been determined by means of ligand ENDOR.

1. Introduction

In our laboratory we are investigating by EPR and ENDOR the magnetic and electric hyperfine interactions in the ground state of S-state ions such as Mn^{2+} and Gd^{3+}, when incorporated in single crystals. One of the quantities, which we are especially interested in, is the spherical electric quadrupole interaction between the nucleus of the paramagnetic S-state ion and its unpaired half-filled shell. Being a free-ion quantity which in the ground state of an ion with a half-filled shell is zero in the non-relativistic limit, this quadrupole interaction is very useful to know for testing relativistic wave functions and many-body perturbation techniques [1]. Using central-ion ENDOR we have shown [2–4] for Gd^{3+} that the above mentioned quadrupole interaction varies only slightly when the ion is incorporated in various host lattices. Since in the case of Gd^{3+} the quadrupole interaction with the half-filled 4f-shell causes shifts in the central-ion ENDOR frequencies which are often an order of magnitude larger than the observed ENDOR linewidths, the corresponding spin Hamiltonian parameter is not all too difficult to determine. However, for Mn^{2+}, which has a half-filled 3d-shell, the situation is somewhat different. The quadrupole interaction in the ground state of the manganese atom has been measured by Evans, Sandars and Woodgate [5] by the accurate method of atomic beam magnetic resonance. From their result it can be estimated that for the Mn^{2+}-ion in a crystalline lattice one should expect ENDOR frequency shifts which are mostly smaller than the frequently occurring ENDOR linewidths. Nevertheless, the present state of art of the ENDOR technique, especially when using higher microwave frequencies (35 GHz) than X-band, encouraged us the perform central-ion ENDOR measurements on Mn^{2+}, with the main purpose of trying to observe the spherical quadrupole interaction in the ^6S ground state.

In this paper we report on the results of central-ion ENDOR measurements on a single crystal of cubic ZnS doped with Mn^{2+}. The reason for taking ZnS: Mn^{2+} was that this system was found to have rather strong central-ion ENDOR signals with relatively small ENDOR linewidths, thus making it possible to measure most of the ENDOR frequencies with an accuracy of about one tenth of the expected maximal shifts due to spherical quadrupole interaction. We also report on the results of ligand ENDOR measurements on Zn^{67}, which has only 4.12% natural abundance. Since we were primarily interested in determining the very small spherical quadrupole interaction of Mn^{55}, the Zn^{67} ENDOR measurements were carried out less rigorously, using only first-order perturbation calculation for the parameter fitting.

Reprint requests to Dr. R. de Beer, Department of Physics, Technische Hogeschool Delft, *Delft*, The Netherlands.

2. ENDOR-Apparatus

The microwave part of the ENDOR apparatus consisted of a home-made Ka-band (35 GHz) superheterodyne spectrometer. The nuclear-resonance field could be provided by three commercial frequency modulated RF oscillators, which together covered a frequency range of 0.1 to 960 MHz. In the lowest

frequency range up to about 50 MHz we used a Hewlett-Packard 8601 A sweep generator, the output of which could be maximally raised to 90 W by an ENI 350 L wideband power amplifier. In the range between 50 and 200 MHz we used a General Radio 1215-C butterfly oscillator combined with a 3 W wideband power amplifier (Instruments for Industry, type M 500). In the highest frequency range the output of 0.2 W of a General Radio 1209-C butterfly oscillator was directly supplied to the nuclear-resonance coil. This coil (one single loop) was placed inside a cilindrical TE_{011} microwave cavity and made part of the inner conductor of the 50 Ω coaxial supply cable. Since the end of this coaxial line was matched to 50 Ω (outside the Dewar vessel) the whole nuclear-resonance system was broadbanded. We had two rotational degrees of freedom to adjust the direction of the external magnetic field with respect to the crystallographic axes of the sample, since the electromagnet could be rotated about its vertical axis and the sample holder about a horizontal axis.

3. Preparation of the Crystal

The crystal was grown by chemical vapour phase transport in a closed silica ampoule from homogeneously doped ZnS:Mn powder with 5 mg I_2/ml as a transport agent. The ampoule was heated in a horizontal tube furnace, keeping the temperature of the growing crystal and the starting material at 700 °C and 900 °C respectively. The crystal grew as a boule with many cracks, from which a clear part was cut for the measurements.

4. Experimental Results

4.1. EPR Measurements

Results of various EPR measurements on natural and synthetic cubic ZnS:Mn^{2+} have been published by several investigators [6–10]. In the case of synthetic cubic ZnS:Mn^{2+} Schneider et al.[10] have shown that due to stacking faults along the $[111]_w$ packing axis the crystals can have two homologous cubic centers, which are related to each other by rotation over 180° about the $[111]_w$ direction. Also an axial center can be present with its axial symmetry axis along $[111]_w$. To our knowledge no liquid helium temperature values for the EPR spin Hamiltonian parameters of cubic ZnS:Mn^{2+} have been reported in the literature. Therefore, we have measured the cubic EPR spectrum at 4.2 K since we needed to know accurately the value of the cubic crystal-field parameter a for the fitting of the ENDOR spin Hamiltonian parameters (all ENDOR measurements were performed at 4.2 K). Like Schneider et al.[10] we also observed the two homologous cubic centers and the axial center. Figure 1 shows the lowest hyperfine group ($M_I = -5/2$) for $\boldsymbol{H}$ parallel to the [001] axis of one of the two cubic systems. The relative intensities of the EPR lines clearly demonstrate the correct assignment of the absolute signs of a and A by Watkins[7]. The broad lines near the central EPR line are due to the second cubic system, the [001] axis of which makes an angle of 70° 32′ with $\boldsymbol{H}$[10].

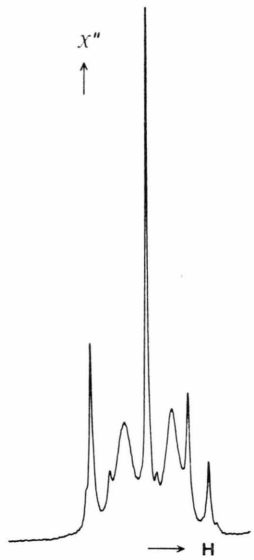

Fig. 1. Lowest hyperfine group ($M_I = -5/2$) of the EPR spectrum of cubic ZnS:Mn^{2+} for $\boldsymbol{H} \parallel [001]$ and $T = 4.2$ K.

4.2. Central-ion ENDOR on Mn^{55}

All ENDOR measurements (also the ligand ENDOR reported later on) were performed with the external magnetic field $\boldsymbol{H}$ in the $(\bar{1}10)_w$ plane (see Figure 2). The samples were oriented with respect to the direction of $\boldsymbol{H}$ (with an accuracy of about $\pm 0.5°$) with the aid of the angular dependence of the axial EPR spectrum. Since for general angles θ between $\boldsymbol{H}$ and $[001]_I$ (the index denotes cubic system I) the EPR spectra of the two cubic systems overlap, the measurements were performed for $\theta = 0°$, 54° 44′ and 144° 44′. For the latter two angles the two cubic EPR spectra coalesce and for $\theta = 0°$ the outer lines of system I are not overlapping with system II (see Figure 1). The following spin Hamiltonian, speci-

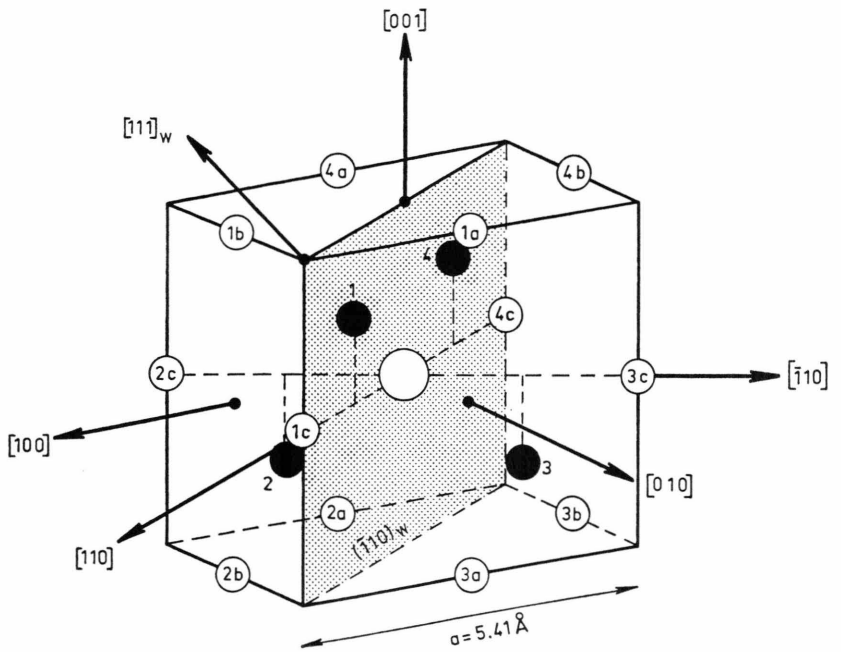

Fig. 2. Nuclear framework of the environment around Mn^{2+} in cubic ZnS. The black circles represent the nearest sulphur ligands and the open circles the next-nearest zinc ligands. The external magnetic field was rotated in the shadowed $(\bar{1}10)_w$ plane.

fied in the crystal coordinate system, was fitted to the ENDOR data

$$\mathcal{H} = g\beta \mathbf{H}\cdot\mathbf{S} + A\,\mathbf{S}\cdot\mathbf{I} + a\{S_4^0 + \sqrt{5/14}\,(S_4^4 + S_4^{-4})\} - g_I\beta_N \mathbf{H}\cdot\mathbf{I} + \frac{Q}{2}\sum_m (-1)^m S_2^m I_2^{-m} + G$$
$$\cdot\left\{S_2^0 I_2^0 + \frac{2}{3}(S_2^1 I_2^{-1} + S_2^{-1} I_2^1) + \frac{1}{6}(S_2^2 I_2^{-2} + S_2^{-2} I_2^2) + \frac{5}{6}(S_2^2 I_2^2 + S_2^{-2} I_2^{-2})\right\}$$
$$+ B\left\{S_3^0 I_1^0 + \frac{\sqrt{6}}{4}(S_3^1 I_1^{-1} + S_3^{-1} I_1^1) + \frac{\sqrt{10}}{4}(S_3^3 I_1^1 + S_3^{-3} I_1^{-1})\right\}$$
$$+ D\left\{S_{zw}^2 - \frac{1}{3}S(S+1)\right\} + P\left\{I_{zw}^2 - \frac{1}{3}I(I+1)\right\}, \qquad (1)$$

where $S = I = 5/2$ and S_l^m and I_l^m are spherical tensor operators. The four first terms in the spin Hamiltonian are conventional. The Q-, G- and B-operators describe the spherical electric quadrupole, the cubic electric quodrupole and the magnetic dipole-octupole interaction respectively. The G-term was first investigated by Woonton and Dyer [11] and the B-term by Ham et al [12]. For the reduced matrix elements we have chosen

$$\langle 5/2 \| I_1 \| 5/2\rangle = \sqrt{210}/2\,,$$
$$\langle 5/2 \| I_2 \| 5/2\rangle = \langle 5/2 \| S_2 \| 5/2\rangle = 4\sqrt{105}\,,$$
$$\langle 5/2 \| S_3 \| 5/2\rangle = 18\sqrt{35}/5\,,$$
$$\langle 5/2 \| S_4 \| 5/2\rangle = 3\sqrt{7}\,.$$

In that case the Q-, G- and B-term are identical to expression (7b), (10b) and (10c) of Woonton and Dyer [11] respectively and the cubic crystal-field term to the well-known expression

$$\frac{a}{6}\left\{S_x^4 + S_y^4 + S_z^4 - \frac{1}{5}S(S+1)(3S^2 + 3S - 1)\right\}.$$

The last two terms in (1) are axial terms, where the index w denotes the $[111]_w$ symmetry axis. We have added these axial terms to the spin Hamiltonian in analogy to the EPR work of Schneider et al [10]. They found that a satisfactory agreement between theory and experiment could only be obtained by adding a small axial crystal-field operator of the type $S_z^2 - \frac{1}{3}S(S+1)$ to the cubic crystal field. This small axial field was assumed to be due to thin hexagonal layers perpendicular to $[111]_w$, caused by the stacking faults. In total 110 central-ion ENDOR frequencies have been used in the fitting of the spin Hamiltonian parameters, 40 belonging to $M_S = -1/2$

(centered around 79 MHz), 40 to $M_S = +1/2$ (around 114 MHz) and 30 to $M_S = -5/2$ (around 470 MHz). The signal to noise ratio and the linewidth of the ENDOR lines (see Fig. 3) as well as the stability of the RF oscillators enabled us to measure most of the frequencies with an accuracy of about ± 0.5 kHz.

Fig. 3. Central-ion ENDOR spectrum of cubic ZnS:Mn^{2+} for $\boldsymbol{H} \| [111]_w$ and $T = 4.2$ K. The spectrum was measured via the $-1/2 \leftrightarrow 1/2$ ($M_I = -3/2$) EPR line. The RF power was 5 W, the time-constant 0.3 s and the magnetic field 12.309 KG. The small lines near the main lines are due to forbidden transitions.

Apart from the electronic g-factor and the cubic crystal-field parameter a, which were kept fixed at their EPR values, the other spin Hamiltonian parameters were fitted to the ENDOR data by means of exact diagonalization of the energy matrix and least-squares adjustment. The values for the adjusted parameters are listed in Table 1. Also listed are the results of the EPR analysis (at 77 K) made by Schneider et al [10]. The agreement between calculated and measured ENDOR frequencies was rather good, the standard deviation of the differences being only about 1 kHz.

4.3. *Ligand ENDOR on Zn^{67}*

In the range of 1.5 to 7 MHz we observed a number of weak ENDOR-lines. The signal to noise ratio being small, RF power up to about 50 W was used. When rotating $\boldsymbol{H}$ in the $(\bar{1}10)_w$ plane the angular diagram of the ENDOR transitions (see Figs. 4 and 5) was found to have a pattern which is charac-

Table 1. Spin Hamiltonian parameters of cubic ZnS:Mn^{2+} as determined by central-ion ENDOR at 4.2 K. The errors in parentheses are three times the standard deviation. Also listed are EPR values as determined at 77 K by Schneider et al. [10].

Parameter		This work ENDOR at 4.2 K	Ref. [10] EPR at 77 K
g		*	2.0022 (3)
A/h	(MHz)	−193.8421 (4)	−193.4 (3)
a/h	(MHz)	24.5 (2) **	23.8 (2)
$g_I \beta_N / h$	(10^{-4} MHz/G)	10.5032 (4)	—
Q/h	(Hz)	−31 (14)	—
G/h	(Hz)	−36 (8)	—
B/h	(kHz)	−1.5 (2)	—
D/h	(MHz)	−9 (3)	−2.8
P/h	(kHz)	0.9 (4)	—

* Not determined, since we have no counter for measuring microwave frequencies of about 35 GHz. In our work the g-value of Ref. [10] was used.
** Determined by EPR.

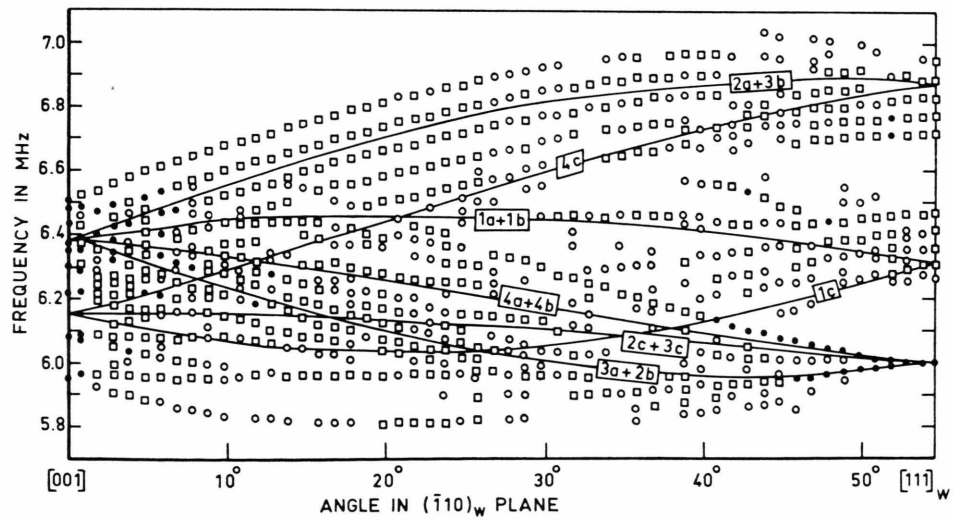

Fig. 4. Angular diagram of the Zn^{67} ENDOR of cubic ZnS:Mn^{2+} for $\boldsymbol{H}$ rotating in the $(\bar{1}10)_w$ plane. The ENDOR lines belong to $M_S = -5/2$ and were measured via the $-5/2 \leftrightarrow -3/2$ ($M_I = -5/2$) EPR line. The solid lines are theoretical curves (see Section 5.2). The full circles, the open circles and the squares denote different ENDOR intensities.

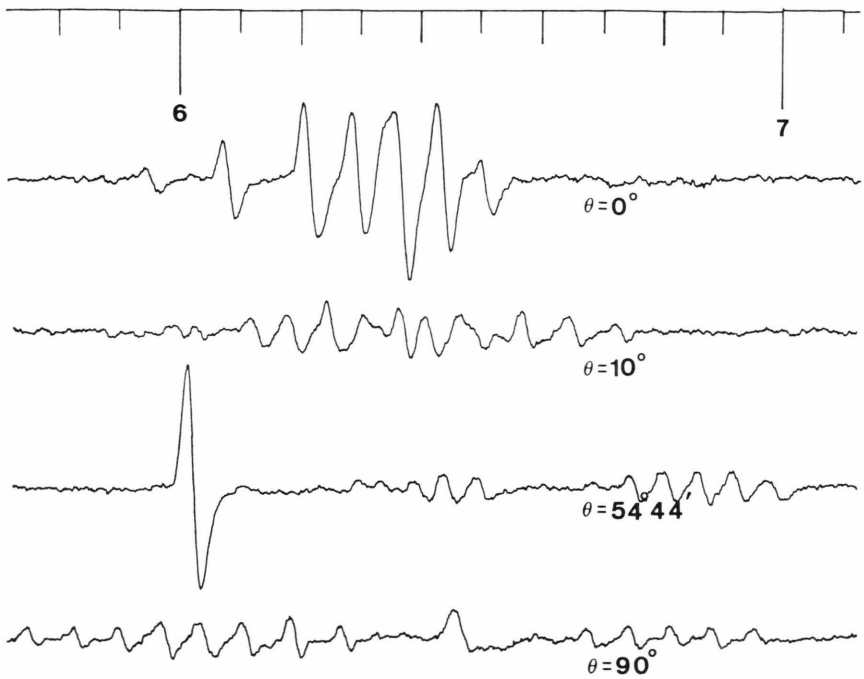

Fig. 5. Zn^{67} ENDOR spectra of cubic ZnS:Mn^{2+} for several angles between $\boldsymbol{H}$ and the [001] axis. The ENDOR lines belong to $M_S=-5/2$. The RF power was about 50 W, the time-constant 3 s and the magnetic field around 12.2 KG.

teristic for nuclei of the {110}-plane class in a lattice of the zinc blende structure [13]. Hence the ENDOR lines could be attributed to the twelve Zn^{67} nuclei nearest to Mn^{2+} (see Figure 2). The major part of the ligand hyperine interaction between Zn^{67} and Mn^{2+} was found to be isotropic. This meant that the ENDOR frequencies were centered around $|\nu_{NMR}-M_S A_i/h|$, where $\nu_{NMR}=2.664\times10^{-4}$ MHz/G for Zn^{67} and A_i is the isotropic hyperfine interaction. In Fig. 6 the dependence on M_S of the

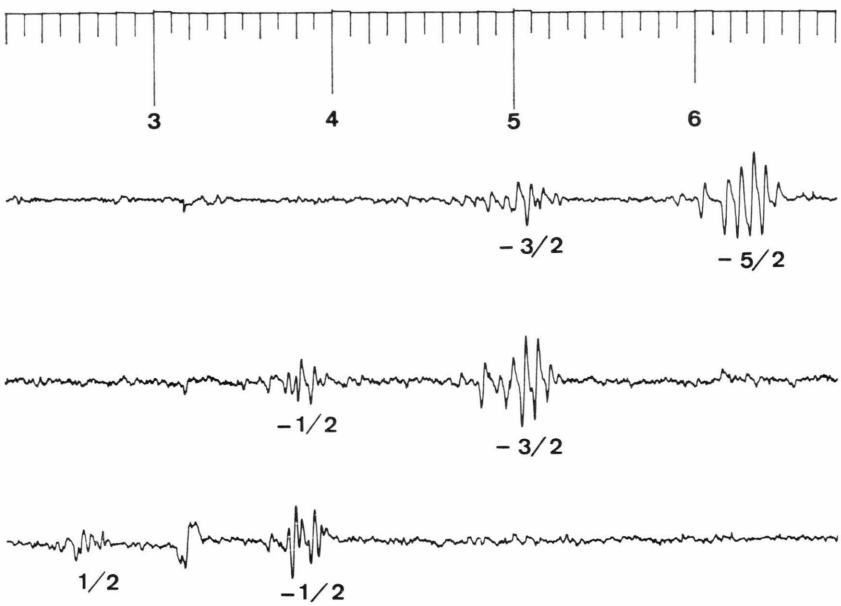

Fig. 6. Dependence of the $H \parallel [001]$ Zn^{67} ENDOR lines on the electronic magnetic quantum number M_S. The spectra were measured via the $-5/2\leftrightarrow-3/2$ ($M_I=-5/2$), the $-3/2\leftrightarrow-1/2$ ($-5/2$) and the $-1/2\leftrightarrow-1/2$ ($-5/2$) EPR line.

ENDOR spectra is shown for the orientation $\boldsymbol{H} \parallel [001]$. It already indicates that A_i/h is positive and of the order of 1 MHz. Using first-order perturbation theory the ligand ENDOR data were interpreted on the basis of the following nuclear spin Hamiltonian

$$\mathcal{H}_N = \sum_n \{ -g_n \beta_N \boldsymbol{H}\cdot\boldsymbol{S} + \boldsymbol{S}\cdot\boldsymbol{A}^n\cdot\boldsymbol{I}_n + \boldsymbol{I}_n\cdot\boldsymbol{P}^n\cdot\boldsymbol{I}_n \}, \quad (2)$$

where $I_n = 5/2$ for Zn^{67}, $n =$ 1a, 2a, ..., 3c, 4c (see Fig. 2), $\boldsymbol{A}^n$ is the ligand hyperfine interaction tensor and $\boldsymbol{P}^n$ the quadrupole interaction tensor. If we specify the tensors in the crystal coordinate system (x along [100], y along [010] and z along [001]) it can be shown [13] for Zn-position 4c that $\boldsymbol{A}^{4c}$ is of the form

$$\boldsymbol{A}^{4c} = \begin{pmatrix} A_i & 0 & 0 \\ 0 & A_i & 0 \\ 0 & 0 & A_i \end{pmatrix} + \begin{pmatrix} -\frac{1}{2}B_{zz} & B_{xy} & B_{xz} \\ B_{xy} & -\frac{1}{2}B_{zz} & B_{xz} \\ B_{xz} & B_{xz} & B_{zz} \end{pmatrix} \quad (3)$$

where the tensor $\boldsymbol{B}^{4c}$ describes the anisotropic part of the ligand hyperfine interaction. It actually means that the z'-axis is along $[\bar{1}10]$ (the prime indicates the principal reference frame of $\boldsymbol{B}^{4c}$). If α_B is the angle between the principal x'-axis and the [001]-axis this angle simply follows from

$$\alpha_B = \tfrac{1}{2}\tan^{-1}\{ -4\,B_{xz}/[\sqrt{2}\,(B_{xx} - B_{zz} + B_{xy})] \}. \quad (4)$$

Analogous to (3) the quadrupole interaction can be written as

$$\boldsymbol{P}^{4c} = \begin{pmatrix} -\frac{1}{2}P_{zz} & P_{xy} & P_{xz} \\ P_{xy} & -\frac{1}{2}P_{zz} & P_{xz} \\ P_{xz} & P_{xz} & P_{zz} \end{pmatrix}. \quad (5)$$

The tensors of the other Zn-nuclei of the nearest {110}-plane shell are related to those of 4c by the symmetry operations of T_d, the site symmetry of Mn^{2+} in ZnS [10]. Table 2 gives A_i, the tensor elements of $\boldsymbol{B}^{4c}$ and $\boldsymbol{P}^{4c}$ and the angles α_B and α_P.

Table 2. Parameters of the ligand hyperfine interaction and the electric quadrupole interaction of the nearest {110}-plane class of Zn^{67} nuclei around Mn^{2+} in cubic ZnS, as determined by ligand ENDOR at 4.2 K. The parameters (and the errors) were calculated by means of first-order perturbation theory.

A_i/h	(MHz)	1.22 (2)
B_{xy}/h	(MHz)	0.18 (2)
B_{xz}/h	(MHz)	0.08 (2)
B_{zz}/h	(MHz)	−0.04 (2)
α_B		69° (1°)
P_{xy}/h	(MHz)	0.000 (4)
P_{xz}/h	(MHz)	∓0.015 (1)
P_{zz}/h	(MHz)	±0.045 (3)
α_P		74° (2°)

The angle α_P defines the direction of the principal x'-axis of $\boldsymbol{P}^{4c}$ in the same way as α_B does for $\boldsymbol{B}^{4c}$. Since the sign of B_{xz} is not determined by the experiment [13] it was chosen in such a way that the principal x'-axis is lying in between the Mn-Zn and the Mn-S internuclear axis. In the first-order calculation of the parameters we only used ENDOR frequencies belonging to the Mn^{2+}-state $|M_S = -5/2, M_I = -5/2\rangle$, which is relatively pure. The same holds for the state $|M_S = +5/2, M_I = +5/2\rangle$, but we could not observe ENDOR lines belonging to $M_S = +5/2$, since for that electronic magnetic quantum number the RF enhancement factor [14]

$$\varepsilon = \{1 - M_S A_i/g_n \beta_N H\}^2$$

is almost zero accidentally.

5. Discussion

5.1. Central-ion ENDOR Parameters

To our knowledge for the first time a value for the spherical electric quadrupole interaction of Mn^{2+} incorporated in a single crystal has been determined. It appears that our value Q (ZnS:Mn^{2+}) $= -31 \pm 14$ Hz is about one third of the value Q (Mn) $= -91 \pm 4$ Hz for the manganese atom, as determined by Evans, Sandars and Woodgate [5] by means of atomic beam magnetic resonance. We do not know whether this difference is due to the influence of the ZnS lattice. To gain information about the "solid-state effect" Mn^{2+} incorporated in other host lattices will be studied experimentally. Furthermore relativistic many-body perturbation calculations are in progress in our laboratory [15] in order to study theoretical the Q of chemically bonded Mn^{2+}. Our (absolute) value for the axial crystalfield parameter D is about three times larger than the value observed by Schneider et al [10], indicating that our samples contained considerably more stacking faults. It is interesting that our value -10.0×10^3 for the ratio D/P is quite different from the values -3.4×10^3 and -1.3×10^3 found for the two manganese sites in $La_2Mg_3(NO_3)_{12} \cdot 24\,H_2O$:$Mn^{2+}$ [16], indicating that there is no clear correlation between D and P. Finally it should be pointed out that although the Q- and G-value seem to be small compared to B and P their effect on the ENDOR frequencies is of the same order of magnitude. This simply depends on the choice of the reduced matrix elements of the spin Hamiltonian operators, because of which the matrix elements of the Q- and G-term are somewhat large compared to the other matrix elements.

5.2. *Ligand ENDOR Parameters*

Although the natural abundance of Zn^{67} is only 4.12% we succeeded in finding ENDOR of the Zn^{67} nuclei nearest to Mn^{2+}. No ENDOR signals of S^{33} could be observed, probably because the natural abundance is even lower (0.74%). The isotropic ligand hyperfine interaction of Zn^{67} as derived from ENDOR is about one half of the value $|A_i/h| = 2.25 \pm 0.15$ MHz, determined by Schneider et al.[10] from superhyperfine structure (SHFS) near the central $-1/2 \leftrightarrow +1/2$ (M_I) EPR lines. We have no explanation for this discrepancy. Unfortunately, we could not repeat the EPR measurements of Schneider et al. since we did not observe any SHFS near our central $-1/2 \leftrightarrow +1/2$ (M_I) EPR lines.

Chen, Kikuchi and Watanabe[17] have expressed the ligand hyperfine interaction tensors for the twelve next-nearest ligands in zinc blende structure crystals in terms of molecular orbital and geometry parameters. Applying their theory (and notation) we can write

$$B_{xx} = A_+ , \quad B_{xy} = A_- , \quad B_{xz} = A_- - 3A_+ \quad (6\,\text{a, b,c})$$

where

$$A_+ = \tfrac{1}{2}(A_M + A_C) , \qquad (7\,\text{a})$$

$$A_- = \frac{3}{2}(A_M + A_C) + A_T . \qquad (7\,\text{b})$$

The sum $(A_M + A_C)$ becomes equal to the point dipole-dipole contribution in the limit of electrostatic bonding. The parameter A_T represents the transfer of unpaired spin density to the sulphur ligands. From (6c), (7a) and (7b) follows that $B_{xz} = A_T$. Hence B_{xz} is a measure for the amount of unpaired spin density at the sulphur sites. It appears that our choice for a positive sign of B_{xz} agrees with the molecular orbital theory [see expression (27) of Chen, Kikuchi and Watanabe[17]]. Applying Eqs. (6a), (6b) and (6c) to the experimental tensor elements (see Table 2) yielded $A_+/h = 0.03 \pm 0.01$ MHz and $A_-/h = 0.18 \pm 0.02$ MHz. With these values and the experimental isotropic interaction we calculated theoretical curves for the angular dependence of the ENDOR lines (see Figure 4). The curves agree reasonably with the experimental central curves of the quadrupole quintets, the mean difference being about ± 0.02 MHz.

Concerning the quadrupole interaction we make the following remarks. According to first-order perturbation theory the quadrupole splitting of the nuclei 2b, 2c, 3a, 3c, 4a and 4b is proportional to P_{xy} for the orientation $\boldsymbol{H} \parallel [111]_w$. The fact that for this direction of $\boldsymbol{H}$ the ENDOR line at 6.00 MHz shows no quadrupole splitting (see Figs. 4 and 5) clearly demonstrates that P_{xy} is zero within experimental accuracy. Our value of α_P ($74^\circ \pm 2^\circ$) seems to be quite reasonable when compared to $\alpha_P = 79^\circ \pm 2^\circ$ reported recently by Teuerle and Hausmann[18] for the nearest {110}-plane class of As^{75} nuclei in the zinc blende lattice of GaAs:Fe^{3+}.

[1] D. van Ormondt and J. Andriessen, to be presented at the sixth International Symposium on Magnetic Resonance, Banff, Alberta, Canada, May 1977.
[2] C. H. Butti, C. A. Swarts, D. van Ormondt, and R. de Beer, J. Magn. Res. **15,** 247 [1974].
[3] D. van Ormondt, M. G. van der Oord, and W. Biesiot, Phys. Letters **55 A,** 54 [1975].
[4] D. van Ormondt, R. de Beer, C. M. de Jong, M. G. van der Oord, M. H. Homs, and H. W. den Hartog, Physica **84 B,** 110 [1976].
[5] L. Evans, P. G. H. Sandars, and G. K. Woodgate, Proc. Roy. Soc. London **A 289,** 108 [1966].
[6] L. M. Matarrese and C. Kikuchi, J. Phys. Chem. Solids **1,** 117 [1956].
[7] G. D. Watkins, Phys. Rev. **110,** 986 [1958].
[8] W. M. Walsh, Phys. Rev. **122,** 762 [1961].
[9] R. S. Title, Phys. Rev. **131,** 623 [1963].
[10] J. Schneider, S. R. Sircar, and A. Räuber, Z. Naturforsch. **18 a,** 980 [1963].
[11] C. A. Woonton and G. L. Dyer, Can. J. Phys. **45,** 2265 [1967].
[12] F. S. Ham, G. W. Ludwig, G. D. Watkins, and H. H. Woodbury, Phys. Rev. Letters **5,** 468 [1960].
[13] E. B. Hale and R. L. Mieher, Phys. Rev. **184,** 739 [1969].
[14] E. R. Davies and T. Rs. Reddy, Phys. Letters **31 A,** 398 [1970].
[15] J. Andriessen, private communication.
[16] R. de Beer and D. van Ormondt, Phys. Letters **27 A,** 475 [1968].
[17] I. Chen, C. Kikuchi, and H. Watanabe, J. Chem. Phys. **42,** 189 [1965].
[18] W. Teuerle and A. Hausmann, Z. Physik **B 23,** 11 [1976].